Effect of SnO_2 Doping on the Performance of High Voltage ZnO Varistors

Bowen Wang[1], Zhiyao Fu[1(✉)], and Anting Kong[2]

[1] State Key Laboratory of Disaster Prevention and Reduction for Power Grid Transmission and Distribution Equipment, State Grid Hunan Electric Power Company Disaster Prevention and Reduction Center, Changsha 410100, China
jxfzy0602@163.com

[2] College of Sciences, Shanghai University, Shanghai 200444, China

Abstract. The effect of the SnO_2 doping on the structure and the electrical performance of ZnO varistors with high voltage was systematically studied. When the doping amount of SnO_2 was small, the main effect was to promote the growth of grains. As the doping amount increased, SnO_2 led to the formation of the Zn_2SnO_4 spinel, inhibiting the growth of ZnO grains. The donor concentration, the boundary barrier and the surface state density decreased first and then increased, respectively. By proper SnO_2 doping, the key performance parameters of the high voltage varistors were improved, where the breakdown voltage gradient was increased from 193.0 to 208.5 $V \cdot mm^{-1}$, the voltage ratio was reduced from 1.74 to 1.73, and the 2 ms square waveform impulse energy withstanding capacity was increased from 200 to 250 A.

Keywords: SnO_2 Doping · ZnO Varistors · Energy withstanding Capacity · Doping Amount

1 Introduction

Zinc oxide varistor is a kind of semiconductor ceramic element made of ZnO as the main material and various additives [1–7]. ZnO varistors have been used for the pro-tection of power transmission and distribution because of their excellent voltage de-pendent property, fast response time and strong energy withstanding capacity [8–12].

Doping can improve the nonlinear voltammetry characteristics of ZnO varistors, increase or decrease grain resistance, promote or inhibit the growth of grains, thus affecting the properties of ZnO varistors [13–17]. Therefore, doping is an important way to improve the performance of ZnO varistors. As a flux, SnO_2 doping can reduce the phase transition temperature of Bi_2O_3 in the sintering process, so as to reduce the potential gradient of the varistors, which is mostly used in low gradient varistors or high energy varistors. Zou Qingwen [18] doped SnO_2 into ZnO varistors and found that the total amount of additives in the new formulation system was significantly decreased, and the protection ability was stronger. Zhijun Xu et. al. [19] investigated the effects of SnO_2

H. Yang et al. (Eds.): SmartGIFT 2022, LNICST 483, pp. 163–172, 2023.
https://doi.org/10.1007/978-3-031-31733-0_15

on the ZnO varistor ceramics. They found that a small amount of SnO_2 caused a high nonlinear coefficient, lower leakage current, as well as noticeably higher breakdown voltage gradient. There have been several reports on the effect of SnO_2 doping on low voltage ZnO varistors, but there are few reports on the influence of SnO_2 doping on the performance, especially on the large energy withstanding capacity of the varistors with high voltage used in power transmission and distribution systems.

Herein, the effect of SnO_2 doping on the properties of the high voltage ZnO varistors was studied in detail. The influence of the doped SnO_2 on the donor concentration, surface density of states, and grain boundary barrier of ZnO varistors was estimated. With appropriate doping amount, the potential gradient, residual voltage ratio and large energy withstanding capacity of the ZnO varistors were enhanced compared to those of the varistors without SnO_2 doping.

2 Experimental Procedure

The ZnO varistor is composed of ZnO (95 mol%) as main material and the other oxides (5 mol%) including Cr_2O_3, Bi_2O_3, Co_2O_3, $MnCO_3$, Sb_2O_3, NiO and SnO_2 (x mol%, x = 0, 0.1, 0.2, 0.3, 0.4, and 0.5) as additives. The samples were named as D0, D1 - 5 according to the content of SnO_2. The ZnO powder and the additive powder were ball milled for 24 h. Centrifugal spray dryer (LZG-5, Wuxi Fenghua Drying Equipment Co., LTD, China) was used for spray granulation of the total slurry. A powder hydraulic press (Y79-25, Shanghai Huci Electric Appliance Development Co., LTD, China) was used for pressing. The green discs were heated to 500 °C to remove organics, then were sintered at 1200 °C to obtain the varistors. Both sides of the sintered samples were coated with Al electrodes.

The crystal phase of the samples was analyzed by an X-ray diffractometer. The morphology of the samples was characterized by a scanning electron microscope. Breakdown voltage U_{1mA}, leakage current I_L, nonlinear coefficient α, and E-J characteristic curve of the samples were measured by a DC varistor parameter tester. The C-V characteristic parameters were tested by a precision impedance analyzer. The donor concentration N_d, the height of the Schottky barrier φ and the surface density N_s were calculated from the C-V plots according to the equation $(\frac{1}{C_b} - \frac{1}{2C_0})^2 = \frac{2(\varphi - V_b)}{q\varepsilon_0\varepsilon_r N_d}$, where C_b is the grain boundary capacitance per unit area, C_0 is the C_b value when the applied bias is 0, and V_b is the bias of the individual grain boundary, φ is the barrier height, q is the charge of an electron, ε_0 and ε_r are the vacuum permittivity and the ZnO relative permittivity, respectively [20, 21]. The aging performance of the varistors was tested by a varistor accelerated aging tester under an AC voltage of $85\%U_{1\,mA}/\sqrt{2}$ at 135 °C for 96 h. The aging performance was evaluated using the aging coefficient K_{ct} ($K_{ct} = P_{96}/P_1$). P_{96} is the power consumption after 96 h, P_1 is the power consumption after 1 h. A K_{ct} value less than 1 indicates a good aging performance.

3 Results and Discussion

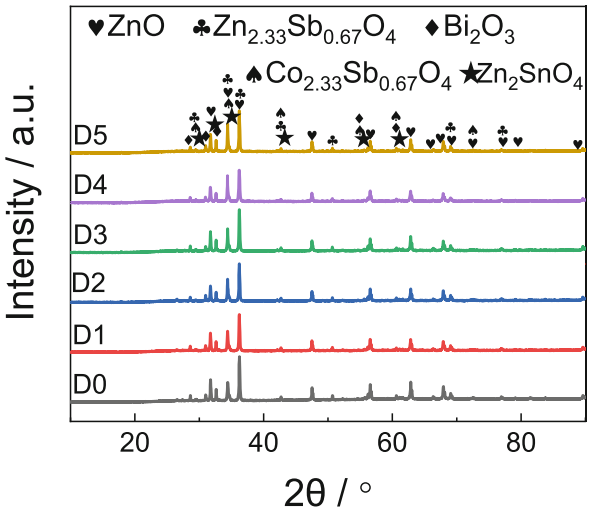

Fig. 1. XRD patterns of ZnO varistors of D0 - D5.

Figure 1 displays the XRD patterns of the ZnO varistors with different SnO_2 doping content. The main structure is composed of hexagonal crystalline ZnO phase, bismuth-rich phase δ-Bi_2O_3 and spinel phases $Zn_{2.33}Sb_{0.67}O_4$ and Zn_2SnO_4. The diffraction patterns of all samples are similar, indicating that SnO_2 does not have a visible effect on the crystal phase of ZnO varistors, which may be because the content of SnO_2 is small.

Figure 2 shows the SEM images of the ZnO varistors with different contents of SnO_2. The average grain size of the sample without SnO_2 was 8.16 μm. With the increase of SnO_2, the grain size increases to 8.98 μm, and then decreases to 7.24 μm. When the doping amount of SnO_2 is small, the main effect is to reduce the phase transition temperature of Bi_2O_3, make the liquid phase form at lower temperature, promoting the grain growth [18]. The grain size distribution of samples D1 - D5 gradually changed from uneven to uniform, and the average grain size gradually decreased, because as the SnO_2 content increased, the inhibiting effect of the spinel on the grain growth was enhanced.

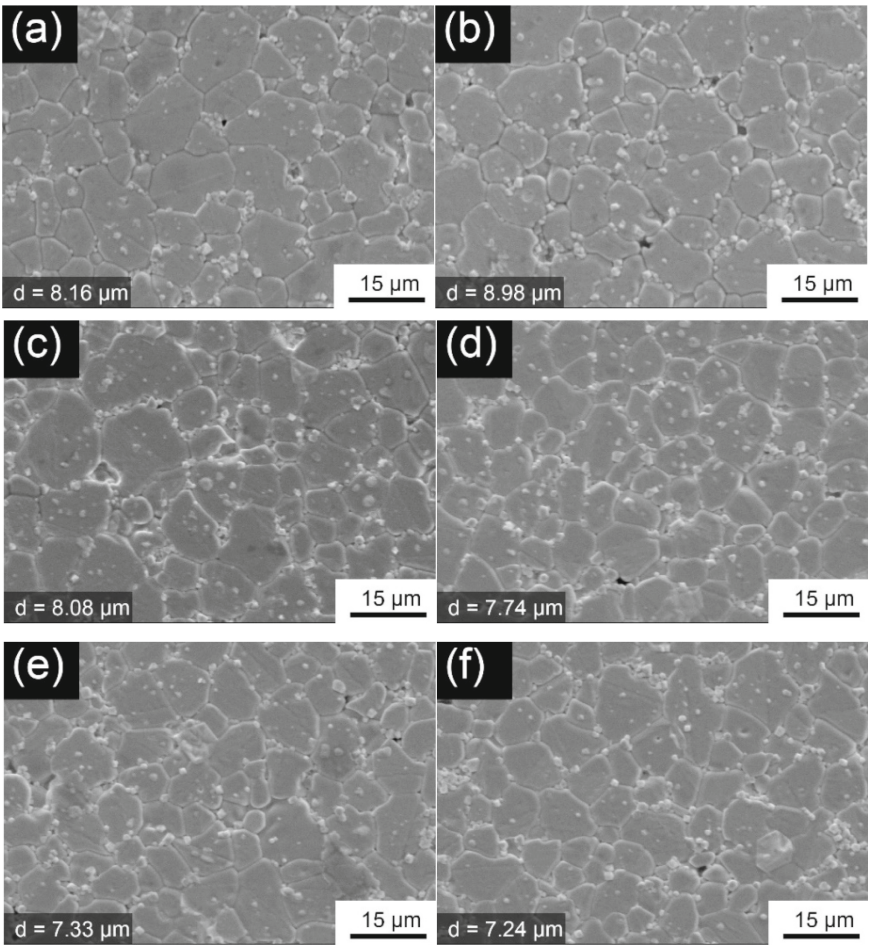

Fig. 2. SEM images of the ZnO varistors of (a) D0, (b) D1, (c) D2, (d) D3, (e) D4, and (f) D5.

Figure 3 (a) shows the potential gradient curves of the ZnO varistors with different amounts of SnO_2 doping. As the SnO_2 amount increases, the potential gradient decreased first from 193.0 to 190.5 $V{\cdot}mm^{-1}$, then increased to 218.9 $V{\cdot}mm^{-1}$. The decrease of the potential gradient is due to the appearance of some voids in the grain and the increase of the grain size. As SnO_2 increases gradually, the grain size decreases and the distribution is uniform, so the potential gradient for D2 - D5 is increasing.

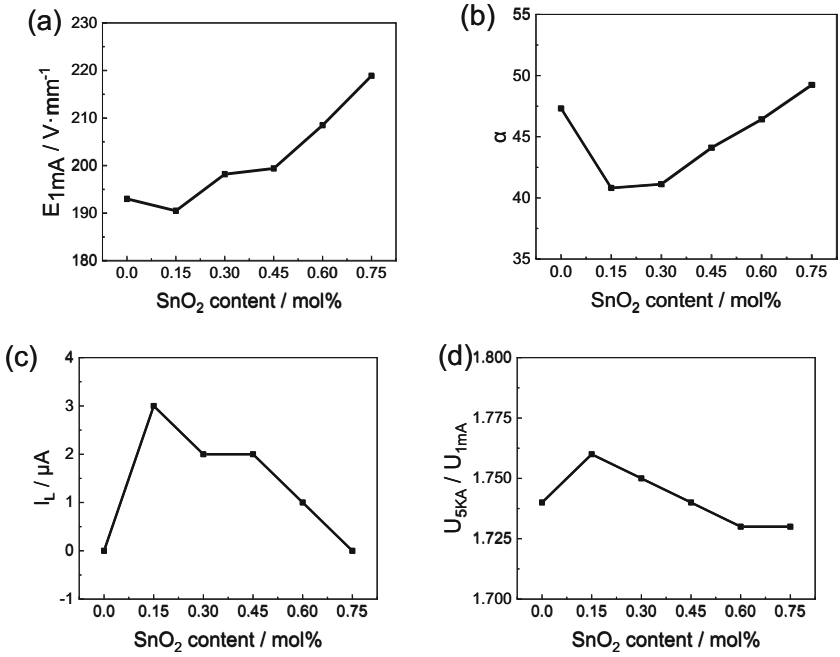

Fig. 3. Properties of ZnO varistors including breakdown voltage gradient (a), nonlinear coefficient (b), leakage current (c) and residual voltage ratio (d) as functions of the SnO_2 content.

Figure 3 (b) displays the variation curve of the nonlinear coefficient of the varistors with different SnO_2 doping contents. With the increasing of the SnO_2 content, the nonlinearity decreases first and then increases. The nonlinear decrease of D1 is due to the lack of spinel particles and uneven distribution. With the increase of the SnO_2 content, the Zn_2SnO_4 spinel was formed on the grain boundary. Spinel particles hindered ion migration and increased the barrier height of the grain boundary.

Figure 3 (c) shows the leakage current curve of the ZnO varistors with different SnO_2 doping contents. With the increase of the SnO_2 content, the leakage current firstly increased and then decreased. According to the formula $J = J_0 exp\left(-v\varphi_B^{\frac{3}{2}}/E\right)$, where J is the current density, J_0 is the current density when the bias is 0, J is inversely proportional to φ, that is, inversely proportional to the nonlinearity [22].

Figure 3 (d) displays the variation of the residual voltage ratio of the ZnO varistors as a function of the SnO_2 doping amount. As the SnO_2 doping amount increases, the residual voltage ratio increased first and then decreased, because E_{5kA} is inversely proportional to E_{1mA}, according to the formula $K = E_{5kA}/E_{1mA}$.

Table 1 shows the detail parameter values of the electrical properties shown in Fig. 3.

Table 1. Electrical properties of the ZnO varistors with different amounts of SnO_2 doping.

Sample	Content (mol%)	E_{1mA} (V/mm^{-1})	α	I_L (μ A)	K (U_{5kA}/U_{1mA})
D0	0	193.0	44.31	0	1.74
D1	0.15	190.5	39.81	3	1.76
D2	0.30	198.2	40.12	2	1.75
D3	0.45	199.4	41.10	2	1.74
D4	0.60	208.5	43.42	1	1.73
D5	0.75	218.9	45.24	0	1.73

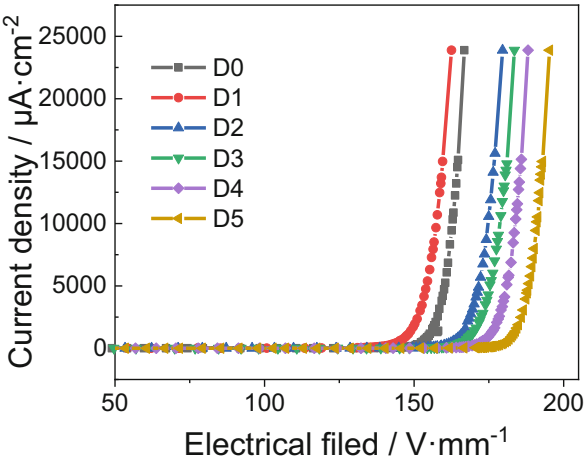

Fig. 4. Electrical field - current density curves of the ZnO varistors with different amounts of SnO_2 doping.

Figure 4 shows the E-J curves of ZnO varistors with different SnO_2 doping contents. The characteristic parameters extracted from the E-J curves are in agreement with those measured by the varistor parameter tester displayed in Table 1, which confirms the validity of the data.

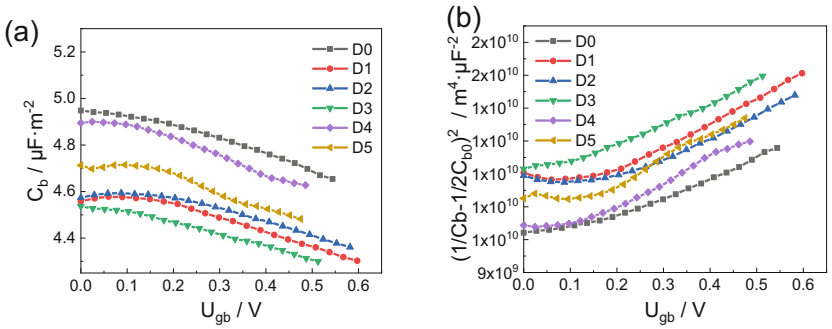

Fig. 5. C-V curves of ZnO varistors with different amounts of SnO_2 doping.

Table 2. Schottky barrier parameters of the ZnO varistors doped with different amounts of SnO_2 doping.

Sample	φ (eV)	N_d(10^{18} m^{-3})	N_s(10^{23} m^{-2})
D0	1.61	2.23	5.73
D1	1.33	1.81	4.72
D2	1.35	1.89	4.87
D3	1.33	1.85	5.16
D4	1.65	2.32	6.61
D5	1.77	2.32	7.09

Figure 5 and Table 2 show the C-V curves of the ZnO varistors and the Schottky barrier characteristic parameters calculated from the curves, respectively. As the SnO_2 content increases, the donor concentration N_d and the surface state density N_s decrease first and then increase, while the grain boundary barrier φ firstly decreases and then increases. The decrease of the donor concentration might because SnO_2 promoted the formation of more liquid phase during sintering, allowing more additives to be incorporated into the Bi-rich phase instead of permeating to ZnO. The increase of N_d and N_s is because Sn^{4+} enters the ZnO lattice and becomes donor doping, increasing the donor concentration. Meanwhile, the oxygen produced by the decomposition of SnO_2 at high temperature increases the partial pressure of oxygen at the grain boundaries, resulting in more surface state density, according to the equation $SnO_2 \leftrightarrow 2Sn_{Zn}^{\cdot\cdot} + 2e' + O_2$.

Figure 6 shows the 2 ms square-waveform energy withstanding capacity of the ZnO varistors with different amounts of SnO_2 doping. As the SnO_2 content increases, the maximum energy withstanding capacity first decreases, then increases to 250 A at sample D4, and then decreases to 200 A at D5. The weakening of the energy withstanding capacity from sample D0 to D1 is due to the uneven grain distribution and more cavities in the ceramic. The improvement of the energy withstanding capacity from D1 to D4 is due to the more uniform grain distribution. The decrease of the energy withstanding capacity from D4 to D5 may be due to the fact that the donor doping has been saturated,

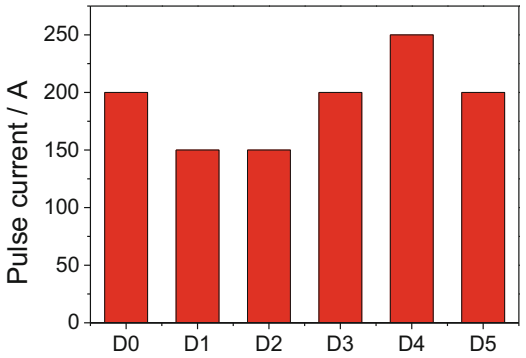

Fig. 6. 2 ms energy withstanding capacity of the ZnO varistors with different amounts of SnO_2 doping.

and the grain resistance cannot further decrease, while the number of grain boundaries further increases, which further aggravates the internal stress.

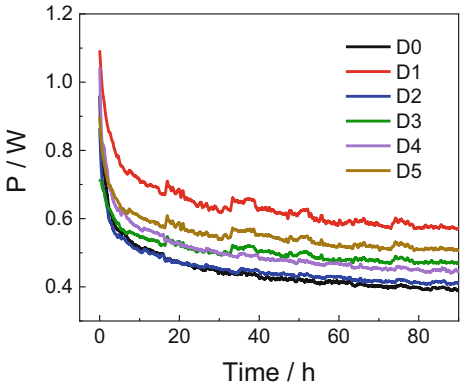

Fig. 7. Accelerated aging performance of the ZnO varistors with different amounts of SnO_2 doping.

In order to verify whether the ZnO varistors can run stably in the circuit, we tested the accelerated aging performance of the samples for 96 h. The accelerated aging curves are shown in Fig. 7, and the performance parameters are displayed in Table 3. The power consumption of D0 - D5 decreases first and then stabilizes as time goes on, and the K_{ct} of all the varistors is less than 1, indicating that all samples can run stably in the circuit. The power consumption is the product of the loading voltage and current of the sample, so the power consumption during aging is roughly proportional to the breakdown voltage gradient and the leakage current [4, 23]. D0 has the second smallest breakdown voltage gradient and the smallest leakage current, thus its aging power consumption is the least. D1 has the smallest breakdown voltage gradient, however, its leakage current is the largest, so its aging power consumption is the largest.

Table 3. Accelerated aging parameters of the ZnO varistors with different amounts of SnO_2 doping.

No	P_{1h} (W)	P_{96h} (W)	K_{ct}
D0	0.77	0.39	0.50
D1	0.97	0.58	0.60
D2	0.73	0.41	0.56
D3	0.69	0.48	0.70
D4	0.85	0.45	0.53
D5	0.77	0.50	0.65

4 Conclusions

This work systematically explored the influence of SnO_2 on the microstructure and the performance of the ZnO varistors. When the doping amount of SnO_2 was small, the main effect was to reduce the phase transition temperature of Bi_2O_3 and promote the ZnO grain growth. As the doping amount increased, SnO_2 led to the formation of the Zn_2SnO_4 spinel, inhibited the ZnO grain growth, promoted the uniform distribution of grains, and improved the uniformity of the structure of the ZnO varistors. During sintering process, Sn^{4+} entered the ZnO lattice, increasing the donor concentration. The oxygen produced by the decomposition of SnO_2 increased the partial pressure of oxygen at the grain boundaries, resulting in more surface state density. Sample D4 has the best comprehensive performance with the potential gradient of 208.5 $V \cdot mm^{-1}$, the nonlinear coefficient of 43.42, the leakage current density of 1 μA, the 5 kA voltage ratio of 1.73, the energy withstanding capacity of 250 A suffering from 18 shocks of 2 ms square waveform pulse impacts, and the ageing coefficient K_{ct} of 0.53.

Acknowledgements. We acknowledge the fund support of Science and Technology Project of State Grid Hunan Electric Power Company (grant 5216AF210004).

References

1. Wang, M., et al.: High improvement of degradation behavior of ZnO varistors under high current surges by appropriate S_b2O_3 doping. J. Eur. Ceram. Soc. **41**(1), 436–442 (2021)
2. Ruan, X., et al.: Effects of dispersant content and pH on dispersion of suspension, microstructures and electrical properties of ZnO varistors. Ceram. Int. **46**(9), 14134–14142 (2020)
3. Liu, W., Zhang, L., Kong, F., Wu, K., Li, S., Li, J.: Enhanced voltage gradient and energy absorption capability in ZnO varistor ceramics by using nano-sized ZnO powders. J. Alloys Compd. **828**, 154252 (2020)
4. Meng, P., Zhao, X., Fu, Z., Wu, J., Hu, J., He, J.: Novel zinc-oxide varistor with superior performance in voltage gradient and aging stability for surge arrester. J. Alloys Compd. **789**, 948–952 (2019)

5. Roy, S., Das, D., Roy, T.K.: Nonlinear electrical properties of ZnO-V_2O_5 based rare earth (Er2O3) added varistors. J. Electron. Mater. **48**(9), 5650–5661 (2019)
6. Zhao, M., Li, X., Li, T.Y., Shi, Y., Li, B.W.: Effect of Y_2O_3, Nd_2O_3 or Sm_2O_3 on the microstructure and electrical properties of ZnVMnNbO varistor ceramics. J. Mater. Sci. Mater. Electron. **30**(1), 450–456 (2019)
7. Roy, S., Roy, T.K., Das, D.: Grain growth kinetics of Er2O3 doped ZnO-V_2O_5 based varistor ceramics. Ceram. Int. **45**(18), 24835–24850 (2019)
8. Zhao, M., Wang, Y.-H., Sun, T.-T., Song, H.-H.: Effect of bismuth and vanadium as the varistor forming element in ZnO-based ceramics. J. Mater. Sci. Mater. Electron. **31**(11), 8206–8211 (2020)
9. Gunnewiek, R.F.K., Perdomo, C.P.F., Cancellieri, I.C., Cardoso, A.L.F., Kiminami, R.H.G.A.: Microwave sintering of a nanostructured low-level additive ZnO-based varistor. Ceram. Int. **46**(10), 15044–15053 (2020)
10. Roy, S., Das, D., Roy, T.K.: Influence of sintering temperature on microstructure and electrical properties of Er_2O_3 added ZnO-V_2O_5-MnO_2-Nb_2O_5 varistor ceramics. J. Alloys Compd. **749**, 687–696 (2018)
11. Meng, P., et al.: Stable electrical properties of ZnO varistor ceramics with multiple additives against the AC accelerated aging process. Ceram. Int. **45**(8), 11105–11108 (2019)
12. Zhao, H., Hu, J., Chen, S., Xie, Q., He, J.: Improving age stability and energy absorption capabilities of ZnO varistors ceramics. Ceram. Int. **42**(15), 17880–17883 (2016)
13. Ruan, X., et al.: Effects of SiO_2/Cr_2O_3 ratios on microstructures and electrical properties of high voltage gradient ZnO varistors. J. Mater. Sci. Mater. Electron. **30**(13), 12113–12121 (2019)
14. Cheng, L.-H., et al.: Electrical properties of Al_2O_3-doped ZnO varistors prepared by sol–gel process for device miniaturization. Ceram. Int. **38**, S457–S461 (2012)
15. Zhu, J., Qi, G., Yang, H., Wang, F.: Microstructure and electrical properties of Pr 6 O 11 doped ZnO-Bi_2O_3-based varistors. J. Mater. Sci. Mater. Electron. **22**(1), 96–100 (2011)
16. He, J., Hu, J., Lin, Y.: ZnO varistors with high voltage gradient and low leakage current by doping rare-earth oxide. Sci. China Ser. E Technol. Sci. **51**(6), 693–701 (2008)
17. Canikoğlu, N., Toplan, N., Yıldız, K., Toplan, H.Ö.: Densification and grain growth of SiO_2-doped ZnO. Ceram. Int. **32**(2), 127–132 (2006)
18. Qingwen, Z.: Study on the amelioration of the formula of ZnO varistor, Xidian University (2012)
19. Shuai, M., Xu, Z., Chu, R., Hao, J., Li, G.: Influence of SnO_2 on ZnO–Bi_2O_3–Co_2O_3 based varistor ceramics. Ceram. Int. **41**(9), 12490–12494 (2015)
20. He, J., Long, W., Hu, J., Liu, J.: Nickel oxide doping effects on electrical characteristics and microstructural phases of ZnO varistors with low residual voltage ratio. J. Ceram. Soc. Jpn. **119**(1385), 43–47 (2011)
21. Wang, X., Ren, X., Li, Z., You, W., Shi, L.: A unique tuning effect of Mg on grain boundaries and grains of ZnO varistor ceramics. J. Eur. Ceram. Soc. **41**(4) (2020)
22. Zhao, H., Hu, J., Chen, S., Xie, Q., He, J.: Tailoring the high-impulse current discharge capability of ZnO varistor ceramics by doping with Ga_2O_3. Ceram. Int. **42**(4), 5582–5586 (2016)
23. Meng, P., et al.: Stable electrical properties of ZnO varistor ceramics with multiple additives against the AC accelerated aging process. Ceram. Int. (2019)